Available online at www.sciencedirect.com
ScienceDirect
Journal of Molecular Catalysis A: Chemical 277 (2007) 193–201
JOURNAL OF MOLECULAR CATALYSIS A: CHEMICAL
www.elsevier.com/locate/molcata

A study of biomimetic system: Exploration of factors modulating the catalytic capacity of glutathione peroxidase mimics

Zeyuan Dong, Kai Liang, Chunyu Wang, Xin Huang, Shizhong Mao, Xiangqiu Li, Jiayun Xu, Junqiu Liu *, Guimin Luo, Jiacong Shen

Key Laboratory for Supramolecular Structure and Materials of Ministry of Education, Jilin University, Changchun 130012, PR China

Received 31 May 2007; accepted 1 August 2007
Available online 9 August 2007

Abstract

A cyclodextrin-based artificial glutathione peroxidase (GPx) system, which was designed to carry single or double binding sites, has been investigated by observing the recognition features of these mimics. The GPx mimics exhibited high catalytic activities mainly due to the substrate recognition generated by hydrophobic driving force. The different recognition mechanisms led to quite different catalytic capacities. In contrast to single recognition, difunctional ones increased the substrate specificity remarkably. The recognition manners of enzyme mimics for substrates strongly depend on the comparative affinities and the concentrations of both substrates. In addition, the catalytic capacity of GPx mimic which contains a delicate binding site for product disulfide can be almost completely blocked via the self-produced inhibition. This work gives very worthful and important information on the understanding of native GPx.

Keywords: Cyclodextrin; Glutathione peroxidases; Hydrophobic interaction; Mimics; Recognition

1. Introduction

Under physiological conditions, reactive oxygen species (ROS) are continuously produced and kept under strict control by many enzymes and antioxidants within the cells [1–6]. As one of antioxidative selenoenzymes, glutathione peroxidase (GPx) displays a strong antioxidant activity and therefore protects the cell membrane and other cellular components from oxidative damage [7–13]. It can scavenge numerous cellular ROS, like hydrogen peroxide, organic hydroperoxides, and phospholipid hydroperoxides, by consuming various reducing substrate such as glutathione (GSH) [7–13]. The active site selenocysteine residue is situated in a hydrophobic pocket on the protein surface [14,15]. According to the computational and experimental findings and suggestions [16–19], the proposed catalytic mechanism of the GPx that involves one ROOH and two GSH is illustrated in Scheme 1, in which these substrates are speculated to consecutively enter the active site and participate in the catalytic reactions. Actually, the exact binding sites of these substrates and their exact binding manners prior to the participation in reactions are not known to date. To understand the mechanism of molecular recognition and catalysis of GPx, we need to know the identities and functions of most of the participants during the catalytic process. Therefore, we employ a kind of GPx mimics (Chart 1) that take advantage of substrate binding sites provided by cyclodextrins, and which are followed with *in vitro* tests of biomimetic systems. Since these GPx mimics show high second-order rate constants for aromatic thiols that are similar to that of some of native GPx (vide infra), the catalysis information obtained by the research of our biomimetic system is reliable to understand the catalytic mechanism of GPx.

Recently, we have successfully fabricated some GPx mimics with a binding site for recognizing substrates [20–23]. In the case of our models, relatively small cyclodextrin-based GPx mimics take advantage of hydrophobic cavities to exhibit strong catalytic capacity and thus are investigated as platforms on the relationships between molecular recognition and catalysis [21,24]. Cyclodextrins can bind hydrophobic substrates to their cavities and have been extensively exploited in the past as enzyme models [25,26]. The interactions of cyclodextrins and substrates are directional, specific, and reversible, and a wealth of information is commonly available on their binding strength and kinetics

* Corresponding author. Fax: +86 431 85193421.
E-mail address: junqiuliu@jlu.edu.cn (J. Liu).

1381-1169/$ – see front matter © 2007 Elsevier B.V. All rights reserved.
doi:10.1016/j.molcata.2007.08.003

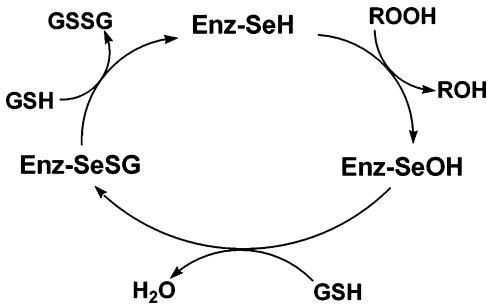

Scheme 1. Experimentally suggested mechanism for the catalytic cycle of GPx.

[25,27]. Previously, the enzyme models based on cyclodextrin monomer, which act on a single bound substrate, showed somewhat low catalytic ability [25]. In order to enhance catalytic ability of enzyme model, improved substrate binding through introducing a second binding site is a promising way. Consequentially, the cyclodextrin dimers have been fabricated and authenticated as excellent enzyme models in which the bifunctional binding of single substrate was demonstrated sufficiently strong [28,29]. However, few receptors designed in such a way to promote the reaction of two simultaneous complexes of substrates were developed so far [30]. Herein, we take advantage of the water-soluble structure with single or double binding sites provided by the cyclodextrins to incorporate catalytic site tellurium for accommodating a model of biomimetic system. Considering the nature of the two-substrate reaction, we choose the formidable peroxidase reaction, partly because the catalytic mechanism of native GPx and the factors for controlling its activity are not fully understood despite the availability of the early detailed experimental information [14,15,20,17,31,32].

In the study, a cyclodextrin-based artificial glutathione peroxidase (GPx) system, which was designed to carry single or double binding sites, has been investigated by observing the recognition features of these mimics through the detailed kinetic and mechanical studies, and very worthful and important information for understanding of native GPx has been given.

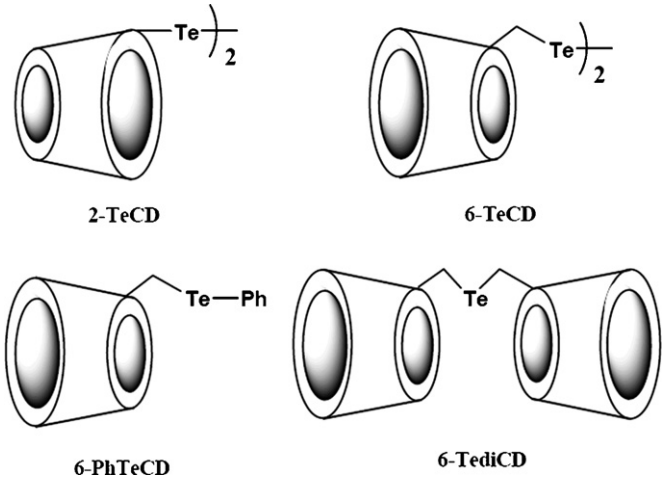

Chart 1. Structures of cyclodextrin-based GPx mimics.

2. Experimental section

2.1. General procedures

Compounds 2,2′-ditellurobis(2-deoxy-β-cyclodextrin) (2-TeCD) [33], 6,6′-ditellurobis(6-deoxy-β-cyclodextrin) (6-TeCD) [34], 6-(phenyltelluro)-6-deoxy-β-cyclodextrin (6-PhTeCD) [35], 6,6′-telluro-bis(6-deoxy-β-cyclodextrin) (6-TediCD) [35], 6,6′-seleno-bis(6-deoxy-β-cyclodextrin) (6-SediCD) [36], 3-carboxyl-4-nitrobenzenethiol (TNB) [37] and di(*p*-nitrophenyl) disulfide (DNBT) [24] were prepared according to the literature procedure and characterized in detail. β-Cyclodextrin was purchased from Tianjin Chemical Plant, recrystallized three times from distilled water, and dried for 12 h at 120 °C in vacuo. *p*-Toluene sulfonylchloride was also purchased from Tianjin Chemical Plant. *tert*-Butyl hydroperoxide (*t*-BuOOH) was purchased from Merck. Cumene hydroperoxide (CuOOH) and 1-adamantaneethanol were purchased from Fluka. Diphenyl ditelluride (PhTeTePh) was obtained from Aldrich. Sodium hydroborate, 5,5′-dithiolbis(2-nitrobenzoic acid) (DTNB), *p*-nitrobenzenethiol (NBT) were purchased from Sigma. All other chemicals were of the highest purity commercially available and were used without further purification. ^{1}H NMR and ^{13}C NMR were measured on a Bruker AM-500 spectrometer. Molecular weight was obtained from a LDI-1700 MALDI-TOF-MS (Linear Scientific Inc., USA). The spectrometric measurements were carried out with a Shimadzu 3100 UV–vis-near-IR Recording Spectrophotometer or Lambda 800 Spectrophotometer interfaced with a personal computer. Data were acquired and analyzed by using ultraviolet spectroscopy software. The temperature for UV time course studies was controlled within (±) 0.5 °C by use of a LAUDA compact low-temperature thermostat RC6 CP. Phosphate buffer (PBS) was used in the all experiments unless otherwise noted. The buffer pH values were determined with a METTLER TOLEDO 320 pH Meter. The concentrations of the hydroperoxide stock solutions were determined by titration with potassium permanganate.

2.2. TNB assay system

The GPx-like activities of these compounds were measured using the Hilvert's method [38,39] with minor modification. The assay mixture contained 50 mM phosphate buffer, pH 7.0, 1 mM EDTA, 100 μM TNB, 250 μM ROOH, and a moderate amount of test compound at 25 °C. Reaction was initiated by the subsequent addition of ROOH and the absorbance at 410 nm (ε = 13,600 M^{-1} cm^{-1}, pH 7.0) was recorded for a few minutes to calculate the reaction rate.

2.3. NBT assay system

The GPx-like activities of these compounds were also assessed using our method [24]. The assay mixture contained 50 mM phosphate buffer, pH 7.0, 1 mM EDTA, 100 μM NBT, 250 μM ROOH, and a moderate amount of test compound at 25 °C. Reaction was initiated by the subsequent addition of

ROOH and the absorbance at 410 nm ($\varepsilon = 14{,}500\ M^{-1}\ cm^{-1}$, pH 7.0) was recorded for a few minutes to calculate the reaction rate.

2.4. Kinetic analysis

The reactions of the reduction of ROOH by NBT in the absence or presence of catalyst were studied by following the disappearance of the thiolate absorption at 410 nm, at pH 7.0 (50 mM phosphate buffer, 1 mM EDTA) and 25 °C. To investigate the dependency of rate on substrate concentration, the reaction rates were determined at several concentration of one substrate while keeping the concentration of the other constant. All kinetic experiments were performed in a solution containing phosphate buffer (50 mM, pH 7.0), ethylendiaminetetraacetate (EDTA, 1 mM), and appropriate concentrations of NBT, ROOH, and test compound. The reaction rates were determined on Shimadzu 3100 UV/Vis-near-IR Recording Spectrophotometer. The reaction was initiated by addition of ROOH. The enzymatic rates were corrected for the background reactions between ROOH and NBT. The initial concentration of NBT was measured from the 410 nm absorbance ($\varepsilon = 14{,}500\ M^{-1}\ cm^{-1}$, pH 7.0). Each initial rate was measured at least five times and calculated from the first 5–10% of the reaction. Lineweaver–Burk plots were obtained by using the Origin 7.0 (professional version) program. For each set of experiments a straight line was drawn with the best-fit method.

2.5. Complexation study of β-cyclodextrin with substrates

We characterized the inclusion complexation of β-cyclodextrin with substrates by means of ^{1}H NMR and UV and fluorescence spectra as well as inhibition experiment [21,24].

2.6. Molecular simulation

We used the molecular modeling program CERIUS^2 4.6 (Accelrys Inc.; San Diego, CA) [40] to carry out our molecular simulation. The Dreiding 2.21 force field from CERIUS^2 software package was used in the entire simulation which had been found to be reliable for many organic systems [41,42]. All of the simulations were started from energy-minimized structures obtained through the Smart Minimizer method and Convergence Level was set to high. The spline function was chosen for switching function in nonbonding interaction. The partial charges were assigned with Charge Equilibration method before each Minimization.

3. Results

3.1. Measurement of GPx-like activities of catalysts by TNB assay system

Thiol TNB exhibits particularly UV spectroscopic properties ($\lambda_{max} = 410$ nm, pH 7.0). Furthermore, the corresponding disulfide does not interfere with the 410 nm absorbance of the thiolate. Therefore, based upon the disappearance of thiolate that can be easily followed spectrophotometrically at 410 nm, the initial rates of the reduction of ROOH (250 μM) by TNB (100 μM) in the presence of various catalysts (1 μM) at pH 7.0 (50 mM PBS, 1 mM EDTA) and 25 °C is determined. Initial rates and relative activities of catalysts are corrected for the respective control rates in the absence of catalyst. In particular, considering the recognition features of GPx mimics, we assume that the relative activity of catalyst is deduced based upon the reaction rate of reduction of H_2O_2 in the presence of corresponding catalyst identically equal to one. The reaction rates and relative activities of these GPx mimics in TNB assay system are shown in Table 1.

3.2. Measurement of GPx-like activities of catalysts by NBT assay system

Like TNB, thiol NBT also exhibits particularly UV spectroscopic properties ($\lambda_{max} = 410$ nm, pH 7.0). Moreover, the corresponding disulfide does not interfere with the 410 nm absorbance of the thiolate. Thus, the initial rates of the reduction of ROOH (250 μM) by NBT (100 μM) in the presence of various catalysts (1 μM) at pH 7.0 (50 mM PBS, 1 mM EDTA) and 25 °C are determined based upon the disappearance of thiolate that can be easily followed spectrophotometrically at 410 nm. Initial rates and relative activities of catalysts are corrected for the respective control rates in the absence of catalyst. In particular, considering the recognition features of GPx mimics, we similarly assume that the relative activity of catalyst is deduced based upon the reaction rate of reduction of H_2O_2 in the presence of corresponding catalyst identically equal to one. The reaction

Table 1
The reaction rates and relative activities of these GPx mimics (1 μM) for the reduction of ROOH (250 μM) by TNB (100 μM) at pH 7.0 (50 mM PBS, 1 mM EDTA) and 25 °C in TNB assay system

Catalyst	v_0[a] (μM min^{-1})			Relative activity		
	H_2O_2	*t*-BuOOH	CuOOH	H_2O_2	*t*-BuOOH	CuOOH
2-TeCD[b]	2.55 ± 0.16	5.45 ± 0.27	24.49 ± 0.94	1.00	2.14	9.61
6-TeCD[c]	0.49 ± 0.03	3.66 ± 0.12	15.01 ± 0.40	1.00	7.47	30.61
6-PhTeCD	0.72 ± 0.04	2.10 ± 0.15	13.07 ± 0.98	1.00	2.93	18.18
6-TediCD	0.026 ± 0.002	6.53 ± 0.51	14.13 ± 1.08	1.00	251.31	543.54

[a] All values are means of at least five times with standard deviation.
[b] Reference [5][5b].
[c] Reference [13].

Table 2
The reaction rates and relative activities of these GPx mimics (1 μM) for the reduction of ROOH (250 μM) by NBT (100 μM) at pH 7.0 (50 mM PBS, 1 mM EDTA) and 25 °C in NBT assay system

Catalyst	v_0[a] (μM min^{-1})			Relative activity		
	H_2O_2	*t*-BuOOH	CuOOH	H_2O_2	*t*-BuOOH	CuOOH
2-TeCD[b]	3.01 ± 0.27	11.50 ± 1.35	44.30 ± 1.46	1.00	5.23	14.30
6-TeCD	0.72 ± 0.09	5.42 ± 0.85	24.40 ± 1.12	1.00	7.53	33.89
6-PhTeCD	0.78 ± 0.03	1.88 ± 0.11	11.35 ± 0.88	1.00	2.39	14.44
6-TediCD	0.034 ± 0.003	6.25 ± 0.47	32.37 ± 1.70	1.00	183.76	951.91

[a] All values are means of at least five times with standard deviation.
[b] Reference [6].

rates and relative activities of these GPx mimics in TNB assay system are shown in Table 2.

3.3. Kinetic and mechanical studies

We had previously reported the detailed kinetic and mechanical studies on the GPx-like catalysis of diorganyl ditellurides, such as 2-TeCD [21,24]. Taking 6-TediCD as an example of diorganyl tellurides, we here investigate their kinetic actions and catalytic mechanism. When the concentration of 6-TediCD is maintained constant while substrate concentration [CuOOH] is increased, a linear increase of rate is found but saturation kinetics are not obtained (Fig. 1). At the same time, when the concentration of 6-TediCD is increased, the rates become very high for higher concentration of CuOOH (data not shown). When the concentration of 6-TediCD is maintained constant while substrate concentration [NBT] is increased, a rapid increase of rate is observed in the initial stages; however, when the substrate concentration is increased further, saturation kinetics are obtained and subsequently the rates slowly decrease (Fig. 2). In order to gauge the catalytic efficiency for the reduction of CuOOH, the apparent kinetic parameters of 6-TediCD were calculated under low NBT concentration: $k_{cat}^{(app)} = 150 \pm 12\,(min^{-1})$, $K_{NBT}^{(app)} = 35 \pm 3\,(\mu M)$, $K_{CuOOH}^{(app)} = 577 \pm 48\,(\mu M)$, $k_{cat}^{(app)}/K_{NBT}^{(app)} = (4.3 \pm 0.2) \times 10^6\,(M^{-1}\,min^{-1})$, $k_{cat}^{(app)}/K_{CuOOH}^{(app)} = (2.6 \pm 0.1) \times 10^5\,(M^{-1}\,min^{-1})$. From these observations above it is clearly shown that the rate of oxidation of 6-TediCD should be the rate-determining step during the catalytic process, which is well consistent with previous suggestions [32,43,44]. Our kinetic studies favor the pervious proposed catalytic mechanism of diorganyl telluride which shuttles between tellurium (II) and tellurium (IV) (Scheme 2) [32,43,44]. Furthermore importantly, the intermediate tellurium (IV) compound, 6-TediCD oxide generated during catalytic process, is isolated and confirmed by MALDI-TOF MS (found 2380.6). Similarly, the intermediate 6-PhTeCD oxide is also isolated and characterized by MALDI-TOF MS (found 1339.3).

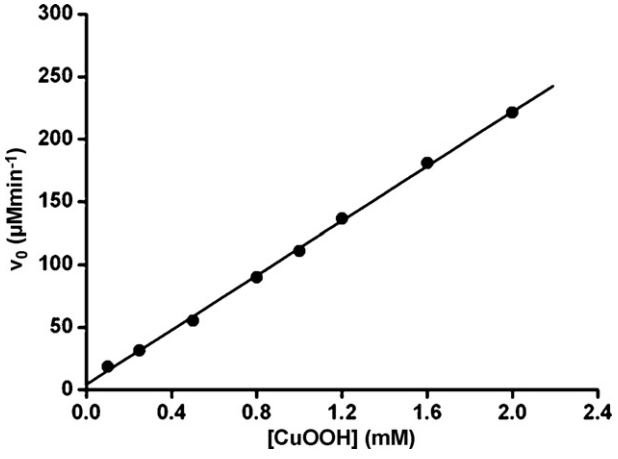

Fig. 1. Plots of the initial rate (v_0) vs. substrate concentration [CuOOH]. The concentrations of catalyst 6-TediCD and thiol NBT was fixed to be 1 μM and 150 μM, respectively, at pH 7.0 (50 mM PBS, 1 mM EDTA) and 25 °C.

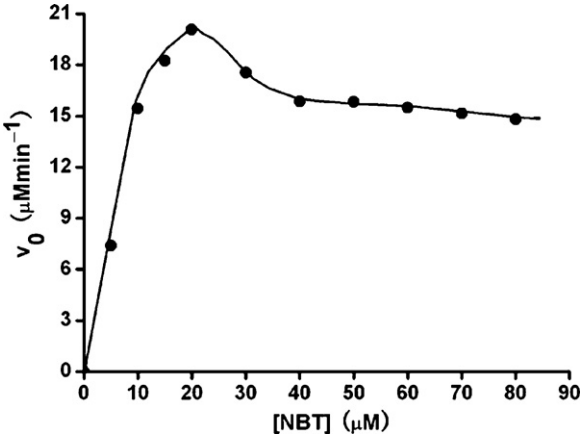

Fig. 2. Plots of the initial rate (v_0) vs. substrate concentration [NBT]. The concentrations of catalyst 6-TediCD and substrate CuOOH was fixed to be 1 μM and 250 μM, respectively, at pH 7.0 (50 mM PBS, 1 mM EDTA) and 25 °C.

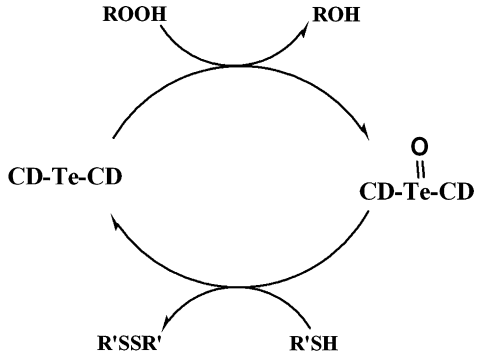

Scheme 2. Proposed catalytic mechanisms for GPx-like reaction of 6-TediCD.

3.4. Complexation study of β-cyclodextrin and substrates

It is long known that cyclodextrins can accommodate hydrophobic substrates to their cavities. Consequently, we measure the complexation affinity of β-cyclodextrin and derivatives with substrates existed in our biomimetic system. The binding constants are used to express the complexation affinity of substrates for GPx mimics. Apparently, hydrophilic H_2O_2 is unfavorable for hydrophobic cyclodextrin cavity. However, the bulky hydrophobic and aromatic CuOOH is favorable for cyclodextrin cavity with a binding constant of $390\,M^{-1}$. The hydrophobic *t*-BuOOH is less suitable for cyclodextrin cavity than CuOOH. The complexation affinities between β-cyclodextrin and ROOH vary in the order K_a(CuOOH) > K_a(*t*-BuOOH) > $K_a(H_2O_2)$. For thiol substrates, aromatic compound TNB is easily bound to the hydrophobic cavity of β-cyclodextrin with a binding constant of $2010\,M^{-1}$. In addition, compound NBT is also easily bound to the hydrophobic cavity with a binding constant of $1860\,M^{-1}$. Indeed, their complexation affinities between β-cyclodextrin and thiols are very close: K_a(TNB) ≈ K_a(NBT).

4. Discussion

To insight into the factors modulating the catalytic capacity of GPx mimics, we make a model of cyclodextrin-based biomimetic system. Since a significant increase in catalytic efficiency of GPx mimic 2-TeCD is obtained by improving the binding affinity of thiol substrate [21,24], it is presented that substrate binding is essential for the catalytic activities of enzymes. As known, the Te–Te bond in ditellurides is easily split by substrates in assay system, the GPx mimics ditellurides such as 2-TeCD exactly have only one binding site to work during the catalytic process. We measure catalytic activities of GPx mimics ditellurides using both direct assay systems, and find that ditellurides show a higher reaction rates using NBT than TNB (Tables 1 and 2). In addition to the difference of the intrinsic reactivities of thiols, we suggest that hydrogen bonding interactions should be responsible for the decreasing rates in TNB assay system because hydrogen bonding interactions played negative roles during catalytic process [24]. In particular, under the experimental conditions 2-TeCD display a rather high reaction rate ($44.30\,\mu M\,min^{-1}$) in the reduction of CuOOH by NBT. During catalysis hydrophobic interactions are the major driving forces of inclusion complexation. The inhibition experiments, using hydrophobic adamantane group as an inhibitor of GPx mimics, further prove the above conclusion [21,24]. It is known that the rates of the background reaction between thiol and ROOH vary in the order $\nu_{contr}(H_2O_2) > \nu_{contr}$(CuOOH) > ν_{contr}(*t*-BuOOH) [21,24,39]. The native β-cyclodextrin has no GPx-like activity in the direct assay system. However, the hydrophobic cavities of catalysts endow these enzyme models with significant ROOH selectivity as evidence that all the rates of the catalyzed reaction in the presence of different ROOH vary in the order ν_0(CuOOH) > ν_0(*t*-BuOOH) > $\nu_0(H_2O_2)$. Interestingly, the enhancement of ROOH binding affinity leads to the increase of Michaelis–Menten constants (K_{thiol}) of 2-TeCD for thiol, indicating the competitive recognition of both substrates for 2-TeCD during catalytic cycle [21]. Of course, these substrates unambiguously compete to occupy the hydrophobic cavities of GPx mimics. As seen in Tables 1 and 2, 6-TeCD displays a lower GPx-like activity than 2-TeCD. The difference of catalytic capacity may be made by geometric preference [21]. This assumption can further be proved by the following observation. When H_2O_2 is used as substrate, 6-TeCD displayed little GPx-like activity ($0.49\,\mu M\,min^{-1}$). However, instead of H_2O_2 by hydrophobic *t*-BuOOH or bulky CuOOH, a larger increase of 7.5-fold and 31-fold, respectively, in reaction rate is observed for 6-TeCD compared to 2-TeCD (2-fold and 10-fold, respectively).

It has been previously demonstrated that diorganyl tellurides can effectively perform the GPx-like functions and hence display antioxidant activities [32,35,43,44]. Expectedly, 6-PhTeCD and 6-TediCD exhibit a significant capacity for catalyzing the peroxidase reaction in the direct assay system. The catalytic mechanism of peroxidase reaction for diorganyl tellurides has been clearly demonstrated (Scheme 2) and differs from that of ditelluride 2-TeCD which may obey the similar catalytic mechanism as that of native GPx (Scheme 1). As observed from Tables 1 and 2, different catalytic mechanism results in different catalytic capacity.

To demonstrate the functions of dual binding sites during catalysis, we follow by a detailed discussion on catalytic capacity of 6-PhTeCD and 6-TediCD. In 6-PhTeCD hydrophobic cavity provided by one cyclodextrin unit endows the molecule with ROOH specificity as evidence that the reaction rates catalyzed the reduction of ROOH by 6-PhTeCD vary in the order ν_0(CuOOH) > ν_0(*t*-BuOOH) > $\nu_0(H_2O_2)$. Particularly, CuOOH was reduced about 10-fold faster than H_2O_2 in the presence of 6-PhTeCD. With single binding site as well as the exposure of catalytic site tellurium, 6-PhTeCD may react with approaching ROOH without steric hindrance caused by structure itself preventing their reaction. However, the compound 6-TediCD, containing two binding sites close to the catalytic site, exhibits a 23-fold decrease in the reaction rate compared to 6-PhTeCD during the reduction of H_2O_2. We conclude that steric hindrance formed by dual cyclodextrin structures in 6-TediCD may be responsible for the rate decrease, besides the fact that the substrate H_2O_2 has no specific affinity for binding sites to approach the catalytic site tellurium. Replacing H_2O_2 by *t*-BuOOH, 6-TediCD exhibits exciting augment of 251-fold in the reaction rate and the highest rate value in the reduction of *t*-BuOOH by TNB among chosen GPx mimics. Most strikingly, instead of H_2O_2 using substrate CuOOH which is favorable for hydrophobic cavity of cyclodextrin, a dramatic enhancement of 952-fold in the reaction rate is observed for 6-TediCD. To our knowledge, this enhancement in catalytic capacity while altering H_2O_2 into CuOOH is rarely observed in all previous GPx model systems. The hydrophobic cavities of 6-TediCD endow this catalyst with very strong ROOH selectivity as evidence that the rates of 6-TediCD-catalyzed reaction in the presence of different ROOH vary in the order ν_0(CuOOH) > ν_0(*t*-BuOOH) ≫ $\nu_0(H_2O_2)$. We think that the difunctional binding sites in the structure of 6-TediCD should be responsible for the exciting change in the reaction rate. In order to nicely clarify the function of

difunctional recognition, we synthesized analogue 6-SediCD and assessed its catalytic capacity by NBT assay system. Unexpectedly, compound 6-SediCD does not give any detectable enhancement in reaction rate while using H_2O_2 as substrate. This result is not surprising because it has been previously reported that some of diorganyl selenides have no any GPx acitivities [13,45]. Interestingly, replacing H_2O_2 by preferential substrate *t*-BuOOH or CuOOH, 6-SediCD exhibits obviously detectable reaction rate (0.71 and 1.12 μM min^{-1}, respectively for 100 μM 6-SediCD). Since 6-SediCD has no any catalytic ability in the presence of H_2O_2, the action of the selenium atom of 6-SediCD can be fully ruled out. This result clearly indicates that the two cyclodextrin moieties of 6-SediCD can cooperatively provide delicate catalytic microenvironment for the specific substrates, such as CuOOH and NBT, and simultaneously bind them to facilitate the peroxidase reaction. Similarly, micelles are also capable of providing nice catalytic microenvironment and then acting as enzyme models [46–49]. However, for hydrophilic H_2O_2 unfavorable for the binding sites, the microenvironment of hydrophobic cavities makes it difficult to be close to binding thiol NBT together. The above result also implies that the structures of cyclodextrin dimers mainly adopt "face to face" conformations. Molecular modeling demonstrates the assumption; in the tube-like structure of 6-TediCD (Fig. 3) the catalytic site tellurium is nearly buried in the interior. From the above observation we believe that substrate binding, in which hydrophobic interactions act as major driving force in complexation, plays an essential role in catalysis. Moreover, the substrate inhibition experiments by adamantane group further confirm this conclusion (data not shown). The difunctional recognition during the catalysis of 6-TediCD endows this molecule with very strong ROOH specificity as observed by the reaction rates (Tables 1 and 2) and large rate acceleration.

To further probe the relationships on the two-substrate recognition and catalysis, kinetic studies of 6-TediCD-catalyzed reduction of CuOOH by NBT are undertaken. In Fig. 2, the decrease of rates can be explained by substrate inhibition at the high NBT concentration. However, substrate CuOOH does not cause inhibition at measured CuOOH concentration range as observed by the catalytic rates (Fig. 1). It seems that the inhibition in catalytic capacity of 6-TediCD strongly depends on the both substrates concentrations as well as their complexation abilities for cyclodextrin cavities. Although the fact that, the binding constant of CuOOH and β-cyclodextrin is approximately five-fold lower than that of NBT, should be responsible for the difference in above kinetic actions, the concentration compensation makes nearly equivalent chance that CuOOH and NBT competitively enter into the binding sites. As observed from Fig. 1, the reaction rate largely increases with increasing the concentration of less specific substrate CuOOH. It is clear that the rate of the catalyzed reaction depends strongly on the concentration of substrate CuOOH or NBT. Very recently, Mugesh and co-workers reported that increasing the substrate concentration can essentially enhance the catalytic capacity of GPx mimic [50]. Although GPx mimic 2-TeCD is not detected any significant inhibition produced by substrates, however, its catalytic efficiency depends strongly upon the competitive recognition of both substrates for 2-TeCD as demonstrated by kinetics analyses [21]. Indeed, for GPx mimic containing only one hydrophobic cavity, two substrates compete each other to occupy the single binding site. However, after introducing a second binding site into GPx mimic, both substrates still rival each other to occupy each of binding sites. Essentially, double binding sites facilitate respective binding of both substrates, and furthermore lower the intensity of competitive recognition of both substrates as observation that, the enhancement of catalytic capacity for 6-TediCD while altering H_2O_2 into CuOOH is far higher than for GPx mimic with single binding site.

Interestingly, the rates of 6-TediCD-catalyzed reaction could also be governed by the product generated during catalytic cycle. Furthermore, the structure and concentration of product are the two major factors that affect the catalytic processes of these GPx mimics. We found that the 6-TediCD-catalyzed reaction can be significantly inhibited by accumulated product DNBT (Fig. 4(A)). It is obvious that the inclusion complexation of DNBT and 6-TediCD is quite strong in the NBT assay system, because 6-TediCD has two cyclodextrin cavities forming nice binding sites suitable for DNBT with an associated constant of far beyond 10^4 M^{-1} [36]. Under the small concentration, product DNBT is incapable of inhibiting the 6-TediCD-catalyzed reaction. When product DNBT accumulates and its concentration increases beyond that of thiol NBT in the assay system,

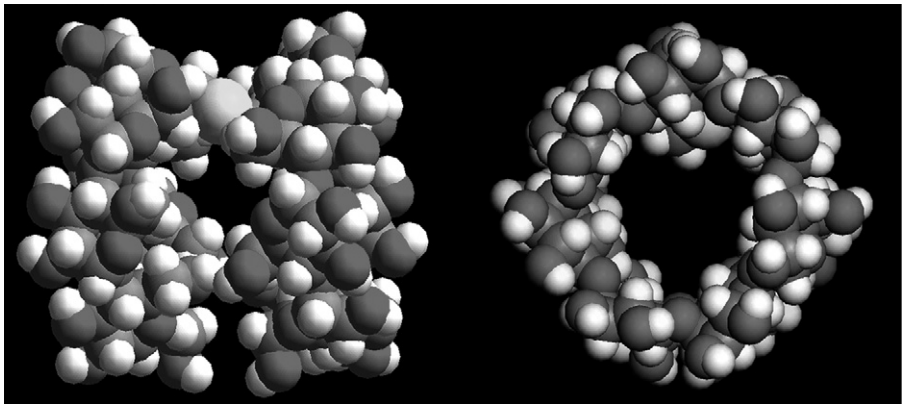

Fig. 3. The side (left) and front view (right) of structure of 6-TediCD.

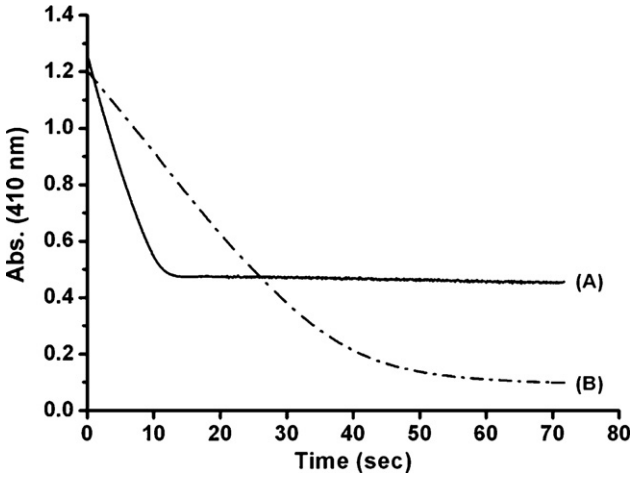

Fig. 4. Plots of Absorbance vs. time (s) monitoring 6-TediCD-catalyzed reaction in direct assay system. (A): NBT assay system; (B) TNB assay system. The thiol concentration [NBT] or [TNB] was 100 μM. The concentrations of catalyst 6-TediCD and substrate CuOOH was fixed to be 10 μM and 250 μM, respectively, at pH 7.0 (50 mM PBS, 1 mM EDTA) and 25 °C.

the catalyzed reaction almost completely stops. The observation not only further demonstrates that the substrate binding is a key factor modulating the large rate accelerations of enzyme, but also suggests that substrate binding is a dynamic process and the concentration factor plays a crucial role during substrate binding of GPx mimic. However, in TNB assay system the 6-TediCD-catalyzed reaction cannot be inhibited by product DTNB (Fig. 4(B)). We found that the concentration of DTNB did not obviously affect the 6-TediCD-catalyzed reaction. Consequently, it is necessary to study the complexing behaviors of product DTNB and 6-TediCD. By means of ^{1}H NMR spectroscopy, we investigated the inclusion complexation of 6-TediCD and product. Very interestingly, we find that the process of inclusion complexation of DTNB and 6-TediCD is dynamically rather slow, and the complexation equilibrium is achieved in at least 1 h (Fig. 5). Like this observation, Harada and co-workers recently also found that a prosthetic group on the end cap of the axle molecule can control the rates of threading of cyclodextrin kinetically [51]. However, the complexation of DNBT and 6-TediCD is too fast to track this process by NMR technology. Therefore in TNB and NBT assay systems, the difference of inhibition phenomena arisen by products is due mainly to the difference of the rates of inclusion complexation of 6-TediCD and products. In Fig. 4(B), it is worth noting that thiol substrate TNB cannot be used up (ca. 6–10% of starting amount) in the presence of excess CuOOH during the catalytic processes of 6-TediCD. Like 6-TediCD, other GPx mimics including 2-TeCD, 6-TeCD, and 6-PhTeCD also cannot extirpate substrates. We conclude that the competitive complexation of substrates and products as well as their binding affinity maybe are responsible for the catalyst-scavenging incompleteness of substrates, which will be expected to be accordant with the keeping physiological balance of ROS by native GPx.

As mentioned above, 6-TediCD displays very high catalytic efficiency with an apparent second-order rate constant

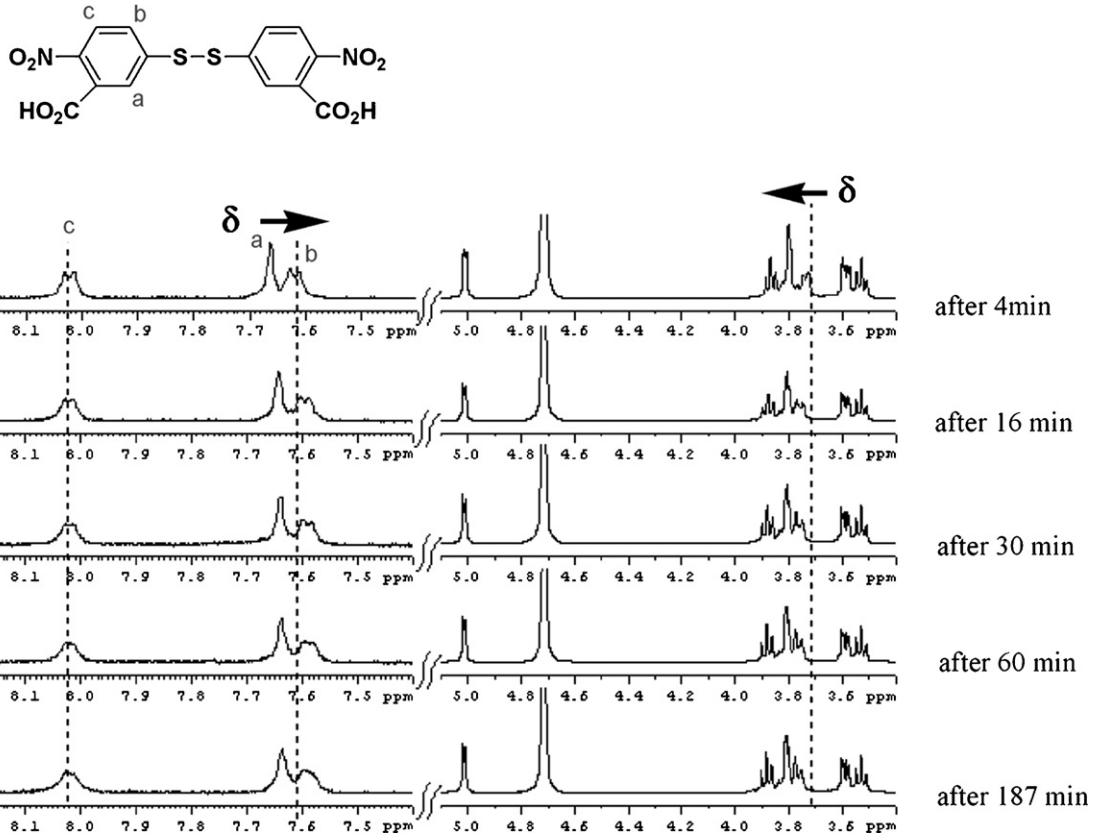

Fig. 5. Comparison of ^{1}H NMR spectra of the complexation of DTNB and 6-TediCD in different time.

of $4.3 \times 10^6\ M^{-1}\ min^{-1}$ for thiol NBT, which is similar to that of native GPx [52]. Since these GPx mimics have quite high second-order rate constants for thiols, the information obtained by our biomimetic system is convincing and available to the suggestions of catalytic mechanism of native GPx. It is well-known that cytosolic GPx exhibits a strong specificity for its thiol substrate GSH, with small structural changes in the thiol leading to large reductions in catalytic capacity [53]. Apparently, substrate binding plays a vital role in GPx catalysis. In addition, the catalytic site selenolate in the natural GPx locates in a shallow depression on the protein surface and may essentially react with any approaching ROOH [54]. In the previous elucidation of structures of GPx, a binding site of product disulfide is assumed through the studies of molecular modeling but not underpinned experimentally [14,15]. We hence suggest that native GPx does not potentially contain a nice binding site for product disulfide via the research of our biomimetic system. Additionally, during catalysis the catalytic ability of GPx would depend on the relative concentrations of reducing and oxidizing substrates.

5. Conclusion

In summary, through the model of biomimetic two-substrate system we find that substrate binding is a key factor modulating the large rate accelerations of enzyme and difunctional recognition effectively accelerates the substrate specificity. Hydrophobic interactions are the primary driving forces during the enzyme-substrate recognition. Moreover, we also demonstrate that during catalysis the recognition manners of enzyme depend on the comparative affinities and concentrations of both substrates. This work provides essential concepts and indications for constructing highly efficient enzyme model as well as important information on the understanding of native GPx.

Acknowledgements

We thank the Natural Science Foundation of China (No. 20534030, 20471023), the National Basic Research Program (2007CB808000), 111 project (B06009), the Innovative Research Team in University (IRT0422), and the Ministry of Education of China for financial support.

References

[1] A.W. Girotti, J. Lipid Res. 39 (1998) 1529.
[2] J. Chaudiere, R. Ferrari-Iliou, Food Chem. Toxicol. 37 (1999) 949.
[3] H. Sies, Oxidative Stress, Academic Press, London, 1985.
[4] C. Rice-Evans, B. Halliwell, G.G. Lunt, Free Radicals and Oxidative Stress: Environment, Drugs and Food Additives, Portland Press, London, 1995.
[5] (a) H. Sies, Exp. Physiol. 82 (1997) 291;
(b) H. Sies, Eur. J. Biochem. 215 (1993) 213.
[6] L.-O. Klotz, K.-D. Kroncke, D.P. Buchczyk, H.J. Sies, Nutrition 133 (2003) 1448.
[7] F. Ursini, M. Maiorino, R. Brigelius-Flohé, K.D. Aumann, A. Roveri, D. Schomburg, L. Flohé, Methods Enzymol. 252 (1995) 38.
[8] R.F. Burk, Selenium in Biology and Human Health, Springer, New York, 1994.
[9] L. Flohé, Curr. Top. Cell Regul. 27 (1985) 473.
[10] A.L. Tappel, Curr. Top. Cell. Regul. 24 (1984) 87.
[11] L. Flohé, G. Loschen, W.A. Günzler, E. Eichele, Hoppe-Seyler's Z. Physiol. Chem. 353 (1972) 987.
[12] T.C. Stadtman, J. Biol. Chem. 266 (1991) 16257.
[13] G. Mugesh, W.-W. du Mont, H. Sies, Chem. Rev. 101 (2001) 2125.
[14] O. Epp, R. Ladenstein, A. Wendel, Eur. J. Biochem. 133 (1983) 51.
[15] B. Ren, W. Huang, B. Åkesson, R. Ladenstein, J. Mol. Biol. 268 (1997) 869.
[16] L. Karen, R. House, B. Dunlap, J.D. Odom, Z.-P. Wu, D. Hilvert, J. Am. Chem. Soc. 114 (1992) 8573.
[17] M. Iwaoka, S. Tomoda, J. Am. Chem. Soc. 116 (1994) 2557.
[18] G. Mugesh, A. Panda, H.B. Singh, N.S. Punekar, R.J. Butcher, J. Am. Chem. Soc. 123 (2001) 839.
[19] G. Mugesh, H.B. Singh, Chem. Soc. Rev. 29 (2000) 347.
[20] G. Luo, X. Ren, J. Liu, Y. Mu, J. Shen, Curr. Med. Chem. 10 (2003) 1151.
[21] Z. Dong, J. Liu, S. Mao, X. Huang, B. Yang, X. Ren, G. Luo, J. Shen, J. Am. Chem. Soc. 126 (2004) 16395.
[22] S. Mao, Z. Dong, J. Liu, X. Li, X. Liu, G. Luo, J. Shen, J. Am. Chem. Soc. 127 (2005) 11588.
[23] H. Yu, J. Liu, A. Bőck, J. Li, G. Luo, J. Shen, J. Biol. Chem. 280 (2005) 11930.
[24] Z. Dong, X. Huang, S. Mao, K. Liang, J. Liu, G. Luo, J. Shen, Chem. Eur. J. 12 (2006) 3575.
[25] R. Breslow, S.D. Dong, Chem. Rev. 98 (1998) 1997.
[26] Y. Murakami, J.I. Kikuchi, Y. Hisaeda, O. Hayashida, Chem. Rev. 96 (1996) 72.
[27] J. Szejtli, Chem. Rev. 98 (1998) 1743.
[28] R. Breslow, B.L. Zhang, J. Am. Chem. Soc. 119 (1997) 1676.
[29] R. Breslow, N. Greenspoon, T. Guo, R. Zarzycki, J. Am. Chem. Soc. 111 (1989) 8296.
[30] R. Cacciapaglia, S.D. Stefano, L. Mandolini, Examples of some catalytic receptors recognizing double substates by hydrogen-bonding interactions, Acc. Chem. Res. 37 (2004) 113.
[31] M. Iwaoka, S. Tomoda, J. Am. Chem. Soc. 118 (1996) 8077.
[32] Y. You, K. Ahsan, M.R. Detty, J. Am. Chem. Soc. 125 (2003) 4918.
[33] X. Ren, Y. Xue, J. Liu, K. Zhang, J. Zheng, G. Luo, C. Guo, Y. Mu, J. Shen, Chem. BioChem. 3 (2002) 356.
[34] Z. Dong, J. Liu, S. Mao, X. Huang, G. Luo, J. Shen, J. Incl. Phenom. Macro. 56 (2006) 179.
[35] M. McNaughton, L. Engman, A. Birmingham, G. Powis, I.A. Cotgreave, J. Med. Chem. 47 (2004) 233.
[36] Z. Dong, X. Li, K. Liang, S. Mao, X. Huang, B. Yang, J. Liu, G. Luo, J. Shen, J. Org. Chem. 72 (2007) 606.
[37] M. Silver, Methods Enzymol. 62D (1979) 135.
[38] Z.P. Wu, D. Hilvert, J. Am. Chem. Soc. 112 (1990) 5647.
[39] I.M. Bell, M.L. Fisher, Z.P. Wu, D. Hilvert, Biochemistry 32 (1993) 3754.
[40] MIS., Molecular Simulation, Inc., Currently Accelrys Inc., San Diego, CA, 1999.
[41] U. Dinur, A.T. Hagler, In Reviews in Computational Chemistry; K.B. Lipkowitz, D.B. Boyd, Ed.; VCH Publishers: New York, 1991; Vol. 2, p. 99.
[42] P. Comba, T.W. Hambley, Molecular Modeling, Weinheim, New York, 1995.
[43] L. Engman, D. Stern, M. Pelcman, C.M. Andersson, J. Org. Chem. 59 (1994) 1973.
[44] T. Kanda, L. Engman, I.A. Cotgreave, G. Powis, J. Org. Chem. 64 (1999) 8161.
[45] S.R. Wilson, P.A. Zucker, R.-R.C. Huang, A. Spector, J. Am. Chem. Soc. 111 (1989) 5936.
[46] R. Svensson, V. Pamedytytė, J. Juodaitytė, R. Makuška, R. Morgenstern, Toxicology 168 (2001) 251.
[47] T. Dwars, E. Paetzold, G. Oehme, Angew. Chem., Int. Ed. 44 (2005) 7174.
[48] X. Huang, Z. Dong, J. Liu, S. Mao, J. Xu, G. Luo, J. Shen, Langmuir 23 (2007) 1518.
[49] X. Huang, Z. Dong, J. Liu, S. Mao, J. Xu, G. Luo, J. Shen, Macromol. Rapid Commun. 27 (2006) 2101.
[50] B.K. Sarma, G. Mugesh, J. Am. Chem. Soc. 127 (2005) 11477.

[51] T. Oshikiri, Y. Takashima, H. Yamaguchi, A. Harada, J. Am. Chem. Soc. 127 (2005) 12186.
[52] G. Takebe, J. Yarimizu, Y. Saito, T. Hayashi, H. Nakamura, J. Yodoi, S. Nagasawa, K. Takahashi, J. Bio. Chem. 277 (2002) 41254.
[53] L. Flohé, W.A. Günzler, G. Jung, E. Schaich, F. Schneider, Hoppe-Seyler's Z. Physiol. Chem. 352 (1971) 159.
[54] L. Flohé, in: D. Dolphin, R. Poulson, O. Avamovic (Eds.), Glutathione: Chemical, Biochemical, and Medical Aspects, Wiley, New York, 1989, p. 644.